

Effect of crumb rubber on compressive behaviour of CRCFST stub columns

Dawei Liu^{1,2}, Jiongfeng Liang^{*1,2}, Guangwu Zhang² and Jianbao Wang²

¹Jiangxi Engineering Research Center of Process and Equipment for New Energy, East China University of Technology, Nanchang, P.R. China

²Faculty of Civil and Architecture Engineering, East China University of Technology, Nanchang, P.R. China

(Received May 18, 2019, Revised February 14, 2020, Accepted February 17, 2020)

Abstract. This paper investigates the effect of crumb rubber (CR) on compressive behaviour of crumb rubber concrete filled steel tube (CRCFST) stub columns. Therefore, experiments on 16 stub columns subjected to axial loading are carried out. The results show that the failure modes of CRCFST stub columns with different CR replacement ratios and CR size are similar, manifested the buckling of the outer steel tube. The axial bearing capacity and stiffness both decrease with an increase in CR replacement ratio, and with decreasing CR size.

Keywords: crumb rubber; concrete; axial; compressive behavior; stub columns

1. Introduction

In recent years, the reuse of waste crumb rubber (CR) as aggregates in concrete has become an effective way to treat waste rubber. And it can help in solving a growing waste tyre challenge, preserving environment. To date, a number of researches have been related to mechanical behavior of crumb rubber concrete (CRC). For example, Murugan and Natarajan (2017) reported the experimental results on mechanical properties, such as compressive strength, split tensile strength and flexural strength, of concrete paving blocks with waste tyre crumb rubber as the fine aggregate. Emiroglu *et al.* (2015) evaluated the dynamic modulus of elasticity of self-consolidating rubberized concrete. Williams and Partheeban (2018) explored the strength prediction of reclaimed rubber concrete by using Genetic Algorithm model. As in previous studies, crumb rubber exhibit better ductility, fire resistance, vibration absorption, shock resistance, explosion resistance, heat insulation and sound insulation (Fu *et al.* 2019, Feng *et al.* 2018, Guo *et al.* 2017). Therefore, several research work have been carried out on the application of CRC in structural members. Youssf *et al.* (2015) found that the hysteretic damping ratio and energy dissipation of the columns enhanced by adding crumb rubber in concrete. Han *et al.* (2015) adopted Xtended Finite Element Method (XFEM) to analyze the fatigue damage of steel and crumble rubber concrete composite beams.

Despite the advantages, the promotion of CRC is restricted by its relatively poorer mechanical properties and reduced workability than those of natural concrete (NC) (Padhi and Panda 2016, Ismail and Hassan 2016). To improve the strength and stiffness of CRC, an effective way is to confine CRC through a steel casing. And Research has

been carried on CRC filled steel tubes. Duarte *et al.* (2018) presented a comparative assessment of rubberized concrete filled square steel tubular columns. The results showed that rubberized concrete filled square steel tubular columns had a marginal higher embodied energy and cost than those of the normal concrete filled square steel tubular column, while the differences were less than 1%. Dong *et al.* (2019) reported that confined rubberised concrete and the restrained steel tube improved ductility of the composite section. The rubberised concrete was more effective in delaying the premature buckling failure of the steel tube compared to the more brittle normal cement concrete. Elchalakani *et al.* (2018) experimentally studied the use of rubberised concrete filled single skin and double skin steel tubes under concentric axial compression. However, the effect of CR on compressive behaviour of crumb rubber concrete filled steel tube (CRCFST) stub columns has rarely been reported.

In this study, the purposes are to present an experimental investigation on the strength and stiffness of CRCFST stub columns with different CR replacement ratio and CR size.

2. Experimental programme

2.1 Materials

Ordinary Portland cement (C) of grade 42.5R, river sand as fine aggregate, crushed stone as coarse aggregate, tap water and crumb rubber were used in this study. And three sizes of particles were selected, namely No. 20 crumb rubber (No. 20 CR) with size fraction of 0.825 mm, No. 40 crumb rubber (No. 40 CR) with size fraction of 0.475 mm and No. 80 crumb rubber (No. 80 CR) with size fraction of 0.18 mm. Sixteen types of concrete mixes were prepared. And a water-to-cement ratio of 0.45 was adopted for all concrete mixes in accordance to Chinese code of JGJ55-2011. In producing crumb rubber concrete (CRC), in place

*Corresponding author, Ph.D.
E-mail: jiongfeng108@126.com



Fig. 1 Crumb rubber

of sand, portions of 0%, 2.5%, 5%, 10%, 20% and 30% CR were added as fine aggregate by mass. The crumb rubber was shown in Fig. 1. Details of concrete mixes are shown in Table 1. Circular steel tubes (Q235) with the height of 456mm, the outer diameter of 114 mm and wall thickness of 2.0 mm were used. Standard tensile coupon tests were conducted to measure material properties of the steel tubes. The measured yield strength (f_y), ultimate strength (f_u) and elastic modulus (E_s) were 382.3 MPa, 441.2 MPa and 202.1 GPa, respectively.

2.2 Specimen design

A total of 16 circular stub columns, including 15 CRCFST stub columns and 1 corresponding normal concrete (NC) filled steel tube stub columns. The main variables investigated in the test are: (a) CR replacement ratio r ($r=0\%$, 2.5%, 5%, 10%, 20%, 30%); (b) CR size (No. 20, No. 40, No. 80, namely, crumb rubber particle size $d=0.825$ mm, 0.475 mm, 0.18 mm). Details of the tested stub columns are presented in Table 2, in which the CRCFST stub column name is a simple concatenation of CR size and CR replacement ratio. For example, a specimen with the label “No.20CR5” represents a circular CRCFST with No. 20 CR size, with 5% of CR replacement ratio.



Fig. 2 Test setup

2.3 Testing

Fig. 2 gives photo of one stub column during testing. The axial compressive load was applied by a universal test machine with a capacity of 3,000 kN. Two linear variable displacement transducers (LVDTs) were used to measure the axial deformation of the test specimen. Four longitudinal strain gauges and four transverse strain gauges were installed at the mid-height and mid-width to measure the strain of the steel tubes, respectively.

3. Results and discussion

3.1 Failure modes

Similar failure behavior is observed for all tested stub columns. In case of specimen No.20CR2.5, there was no obvious change in the appearance of tested specimens in the

Table 1 Mix proportion of crumb rubber concrete

No.	r (%)	No.20 CR (kg·m ⁻³)	No.40 CR (kg·m ⁻³)	No.80 CR (kg·m ⁻³)	Cement (kg·m ⁻³)	Sand (kg·m ⁻³)	Crushed stone (kg·m ⁻³)	Water (kg·m ⁻³)
NC	0	0	0	0	422	531	1257	190
No.20CR2.5	2.5	13	0	0	422	518	1257	190
No.20CR5	5	27	0	0	422	504	1257	190
No.20CR10	10	53	0	0	422	478	1257	190
No.20CR20	20	106	0	0	422	425	1257	190
No.20CR30	30	159	0	0	422	372	1257	190
No.40CR2.5	2.5	0	13	0	422	518	1257	190
No.40CR5	5	0	27	0	422	504	1257	190
No.40CR10	10	0	53	0	422	478	1257	190
No.40CR20	20	0	106	0	422	425	1257	190
No.40CR30	30	0	159	0	422	372	1257	190
No.80CR2.5	2.5	0	0	13	422	518	1257	190
No.80CR5	5	0	0	27	422	504	1257	190
No.80CR10	10	0	0	53	422	478	1257	190
No.80CR20	20	0	0	106	422	425	1257	190
No.80CR30	30	0	0	159	422	372	1257	190

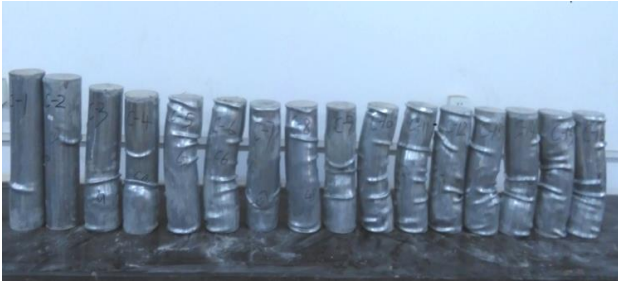


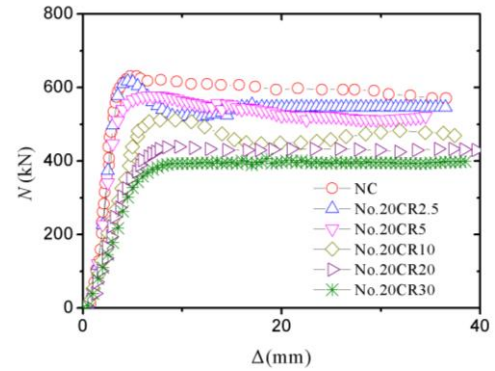
Fig. 3 Failure modes

initial stage, the specimens were in the elastic stage, and the deformation was very small; as the load continued to increase, the strain of steel tube increased growly, and the steel tubes began to buckle; after entering the elastic-plastic stage, the longitudinal deformation of the specimens and the strain of the steel tube increased rapidly; when the load attained the maximum load, multiple outward local buckling appeared; finally, all specimen failed in waist drum oblique shear compression manner. The failure mode of all stub columns is shown in Fig. 3. It can be seen that there are no obvious difference in the failure modes for different stub columns except that more local buckling appeared in the columns with crumb rubber. The reason may be that the crumb rubber concrete (CRC) shows high ductility than natural concrete (NC), in the sense that NC starts expanding due to crushing and cracking earlier than CRC. It resulted in larger ductility for CRCFST stub columns.

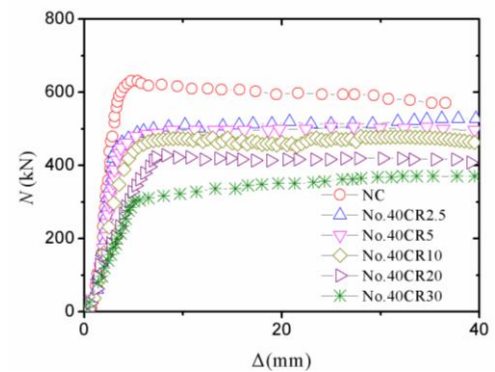
3.2 Axial load-deformation relationships

Fig. 4 presents the influences of CR replacement ratio on axial load (N)-deformation (Δ) relationships of CRCFST stub columns. It is obviously that the formation of N - Δ curves of CRCFST stub columns with different CR replacement ratio was similar to each other. The curves exhibited basically a tendency of rising, falling or gentle, which was still into elastic stage, elastic-plastic stage, plastic stage and downward stage or gentle stage. And the N - Δ curves at the initial stage of loading had a good linear increasing relationship, and then the N - Δ curves were non-linear until the ultimate load was reached. Subsequently, the load decreased with the development of deformation or entered the gentle section, and the deformation developed rapidly at this stage. But the circular steel tubes filled with NC had higher load carrying capacity than those filled with CRC. And generally, the descending portion of N - Δ curves of CRCFST stub columns was more flat than that of CFST stub columns.

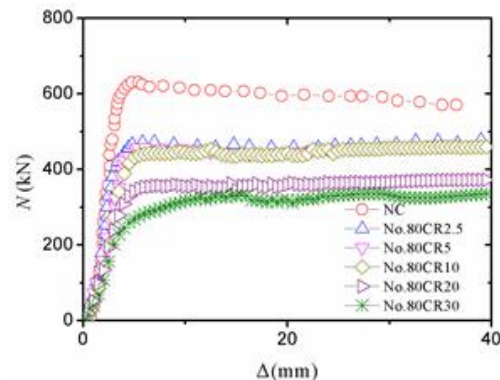
Fig. 5 presents the influences of CR size on axial load (N)-deformation (Δ) relationships of CRCFST stub columns. It was found that there were no noticeable differences in the shape of N - Δ curves of CRCFST stub columns with different CR size. However, the N - Δ curves of CRCFST stub columns with large CR size were higher than those stub columns with small size. That was, the load carrying capacity of No. 20 CRCFST stub columns at given the same CR replacement ratio was higher than that of No. 40 CRCFST stub columns and No. 80 CRCFST stub



(a) No. 20CR stub columns



(b) No. 40CR stub columns



(c) No. 80CR stub columns

Fig. 4 Axial load-deformation relationships of CRCFST stub columns with different CR replacement ratio

columns. And with decreasing CR size (i.e., increasing size fraction of CR), the elastic stage of the N - Δ curves became shorter and the elastic-plastic stage turned much longer. For instance, the N - Δ curves of No. 40 CRCFST stub columns had much longer elastic stage and shorter elastic-plastic stage than that of No. 20 CRCFST stub columns. Moreover, the improved ductility of the CRC filled steel tubes can be observed in Fig. 4 and Fig. 5 as the peak of NC filled steel tube was sharper compared to that of CRCFST.

3.3 Axial load carrying capacity

To evaluate the axial load carrying capacity of CRCFST stub columns, a strength index (SI) is defined as shown in Eq. (1)

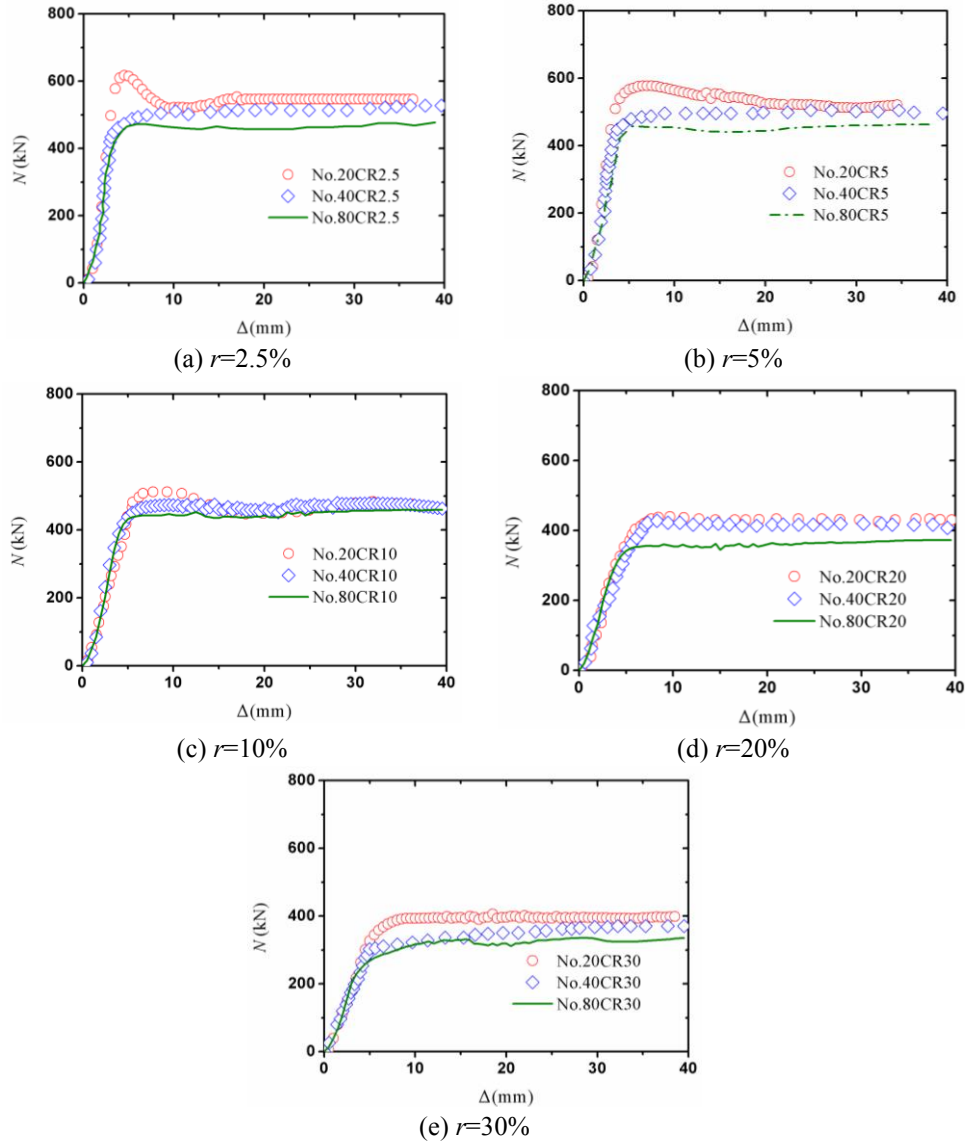


Fig. 5 Axial load-deformation relationships of CRCFST stub columns with different CR size

$$SI = \frac{N_{ucr}}{N_{uc}} \quad (1)$$

Where N_{ucr} is axial load carrying capacity of a CRCFST stub column, N_{uc} is axial load carrying capacity of a NACFST stub column. Fig. 6 shows the SI of CRCFST stub columns with different CR replacement ratio. The ranges of the SI for No. 20, No. 40 and No. 80 CRCFST stub columns were 0.623-0.978, 0.537-0.803, and 0.528-0.731, respectively. This illustrated that the circular steel tubes filled with CRC showed lower axial load carrying capacity than circular steel tubes filled with NC. And the axial load carrying capacity of CRCFST stub column decreased with an increase in CR replacement ratio. For example, SI of No. 20CR2.5, No. 20CR5, No. 20CR10, No. 20CR20 and No. 20CR30 stub columns decreased by 2.2%, 8.6%, 18.9%, 31.9%, 37.7% in comparison with NC stub columns, respectively. The reason is that addition of CR reduced the compressive strength of concrete, which could make the axial load carrying capacity of stub column decreased.

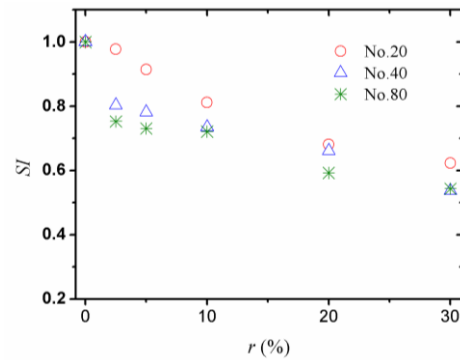


Fig. 6 SI of CRCFST stub columns with different CR replacement ratio

Fig. 7 shows the SI of CRCFST stub columns with different CR size. It clearly indicates that the SI decreased as CR size decreased. For example, the SI values of No.20, No. 40 and No. 80 CRCFST stub columns with 5% CR replacement ratio were 0.914, 0.781 and 0.731, respectively.

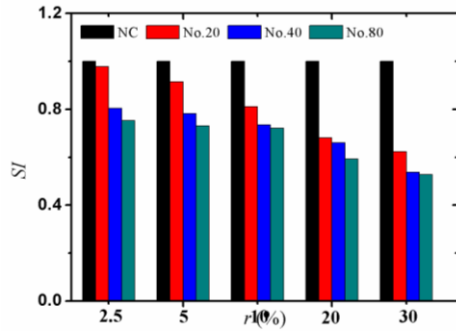


Fig. 7 SI of CRCFST stub columns with different CR size

In other words, the larger the CR size, the higher the axial load carrying capacity of CRCFST stub column. This is attributed to the fact that adding large CR size in concrete had higher compressive strength than adding small CR size, and a higher compressive strength of concrete leads to a higher axial load carrying capacity.

According to the measured data, the empirical formulae of SI with respect to CR replacement ratio (r) and CR particle size (d) is given, as follow

$$SI = 1 - 0.015r - 0.066d \quad (2)$$

Fig. 8 shows comparison between calculated and measured SI. It can be seen that the calculated results agree basically with the measured results. However, it should be noted these formulae are generated based on sixteen limiting values only.

3.4 Stiffness

Similarly, a stiffness index (KI) is defined to quantify the initial stiffness of CRCFST stub columns as follows

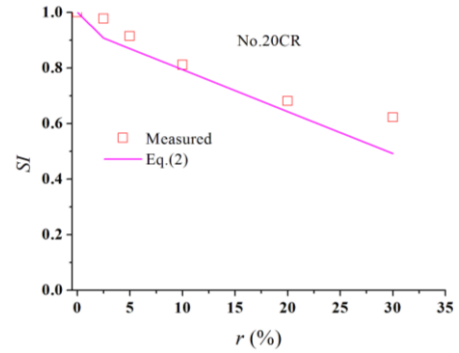
$$KI = \frac{K_{cr}}{K_c} \quad (3)$$

where K_{cr} , K_c are the secant stiffness corresponding to the CRC filled steel tubes stub columns and NC filled steel tubes stub columns, respectively. Here, the secant stiffness (K) can be calculated using Eq. (4) suggested by Yang *et al.* (2013).

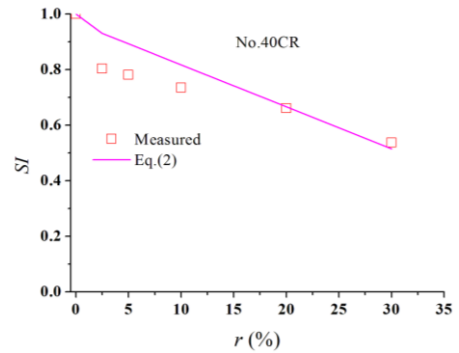
$$K = \frac{0.4N_u}{\epsilon_{0.4}} \quad (4)$$

Where N_u , $\epsilon_{0.4}$ are the maximum load and the axial strain corresponding to the load of $0.4N_u$, respectively.

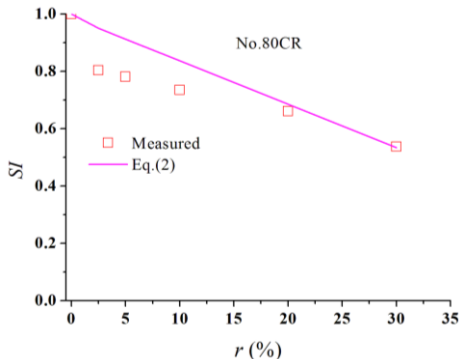
Fig. 9 shows the KI of CRCFST stub columns with different CR replacement ratio. The KI for No. 20, No. 40 and No. 80 CRCFST stub columns was in the ranges of 0.443-0.945, 0.439-0.879, and 0.445-0.789, respectively. It is evident that KI of the stub columns declines due to addition of CR. And with increasing CR replacement ratio, KI of CRCFST stub columns decreased. For No.40 CRCFST stub columns, KI decreased by 56.1% as CR replacement ratio r increased by 30% (from 0% to 30%). Fig. 10 shows the KI of CRCFST stub columns with different CR size. It can be seen that KI for CRCFST stub columns with large CR size was larger than that for



(a) No.20CR CRCFST stub columns



(b) No.40CR CRCFST stub columns



(c) No.80CR CRCFST stub columns

Fig. 8 Comparison between calculated and measured SI

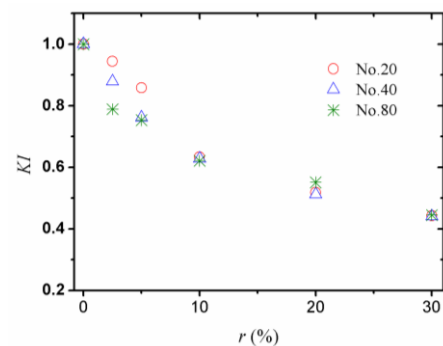


Fig. 9 KI of CRCFST stub columns with different CR replacement ratio

CRCFST stub columns with small CR size when the CR replacement ratio was the same. Above all, it indicated that the CR replacement ratio and CR size have larger influence on stiffness of CRCFST stub columns.

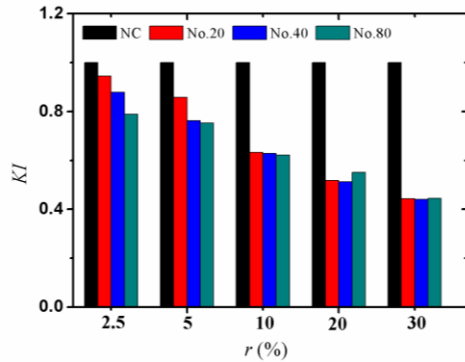


Fig. 10 KI of CRCFST stub columns with different CR size

4. Conclusions

Based on the experimental results, the following conclusions can be drawn:

- (1) The CRC filled steel tubes generally delayed the fracture of the steel tubes compared to NC, which resulted in larger ductility for CRCFST stub columns. However, the failure modes of CRCFST stub columns with different CR replacement ratios and CR size were similar to that of normal CFST stub columns. They failed by buckling of the outer steel tube.
- (2) The descending portion of axial load-deformation curves of CRCFST stub columns was more flat than that of normal CFST stub columns. And the formation of axial load-deformation curves of CRCFST stub columns with different CR replacement ratio and CR size was similar to each other. The elastic stage of the axial load-deformation curves became shorter and the elastic-plastic stage turned much longer with decreasing CR size.
- (3) CRCFST columns exhibited higher ductility than CFST columns, but also lower stiffness and axial load carrying capacity. The axial load carrying capacity and initial stiffness of CRCFST stub columns declined with increasing CR replacement ratio or decreasing CR size.

Acknowledgments

This work was supported by the Chinese National Natural Science Foundation (No. 51868001), the Natural Science Foundation of Jiangxi Province (No.20142BAB216002), the Technology Support Project of Jiangxi Province (No. 20161BBH80045), and the Open Project Program of Jiangxi Engineering Research Center of Process and Equipment for New Energy, East China Institute of Technology (No. JXNE-2014-08), which are gratefully acknowledged.

References

Dong, M., Elchalakani, M., Karrech, A., Hassanein, M.F., Xie, T. and Yang, B. (2019), "Behaviour and design of rubberised concrete filled steel tubes under combined loading conditions",

- Thin Wall Struct.*, **139**, 24-38. <https://doi.org/10.1016/j.tws.2019.02.031>.
- Duarte, A.P.C., Silvestre, N., de Brito, J., Julio, E. and Silvestre, J.D. (2018), "On the sustainability of rubberized concrete filled square steel tubular columns", *J. Clean Prod.*, **170**, 510-521. <https://doi.org/10.1016/j.jclepro.2017.09.131>.
- Elchalakani, M., Hassanein, M.F., Karrech, A. and Yang, B. (2018), "Experimental investigation of rubberised concrete-filled double skin square tubular columns under axial compression", *Eng. Struct.*, **171**, 730-746. <https://doi.org/10.1016/j.engstruct.2018.05.123>.
- Emiroglu, M., Yildiz, S. and Kelestemur, M.H. (2015), "A study on dynamic modulus of self-consolidating rubberized concrete", *Comput. Concrete*, **15**(5), 795-805. <https://doi.org/10.12989/cac.2015.15.5.795>.
- Feng, W., Liu, F., Yang, F., Li, L. and Jing, L. (2018), "Experimental study on dynamic split tensile properties of rubber concrete", *Constr. Build. Mater.*, **165**, 675-687. <https://doi.org/10.1016/j.conbuildmat.2018.01.073>.
- Fu, C., Ye, H., Wang, K., Zhu, K. and He, C. (2019), "Evolution of mechanical properties of steel fiber-reinforced rubberized concrete (FR-RC)", *Compos. Part B-Eng.*, **160**, 158-166. <https://doi.org/10.1016/j.compositesb.2018.10.045>.
- Guo, S., Dai, Q., Si, R., Sun, X. and Lu, C. (2017), "Evaluation of properties and performance of rubber-modified concrete for recycling of waste scrap tire", *J. Clean Prod.*, **148**, 681-689. <https://doi.org/10.1016/j.jclepro.2017.02.046>.
- Han, Q.H., Yang, G., Xu, J. and Wang, Y.H. (2017), "Fatigue analysis of crumble rubber concrete-steel composite beams based on XFEM", *Steel Compos. Struct.*, **25**(1), 57-65. <https://doi.org/10.12989/scs.2017.25.1.057>.
- Ismail, M.K. and Hassan, A.A.A. (2016), "Performance of full-scale self-consolidating rubberized concrete beams in flexure", *ACI Mater. J.*, **113**(2), 207-218. <https://doi.org/10.14359/51688640>.
- Murugan, R.B. and Natarajan, C. (2017), "Investigation on the use of waste tyre crumb rubber in concrete paving blocks", *Comput. Concrete*, **20**(3), 311-318. <https://doi.org/10.12989/cac.2017.20.3.311>.
- Padhi, S. and Panda, K.C. (2016), "Fresh and hardened properties of rubberized concrete using fine rubber and silpozz", *Adv. Concrete Constr.*, **4**(1), 49-69. <https://doi.org/10.12989/acc.2016.4.1.049>.
- Specification for Mix Proportion Design of Ordinary Concrete (JGJ 55-2011) (2011), China Architecture and Building Press, Beijing, China. (in Chinese)
- Williams, K.C. and Partheeban, P. (2018), "An experimental and numerical approach in strength prediction of reclaimed rubber concrete", *Adv. Concrete Constr.*, **6**(1), 87-102. <https://doi.org/10.12989/acc.2018.6.1.087>.
- Youssf, O., ElGawady, M.A. and Mills, J.E. (2015), "Experimental investigation of crumb rubber concrete columns under seismic loading", *Struct.*, **3**, 13-27. <https://doi.org/10.1016/j.istruc.2015.02.005>.

CC